CARDIAC IMAGING

Iran J Radiol. 2017 April; 14(2):e42272. doi: 10.5812/iranjradiol.42272.

Published online 2017 January 1. **Research Article**

Left Ventricle Segmentation Using a Combination of Region Growing and Graph Based Method

Mostafa Ghelich Oghli,[1] Maryam Mohammadzadeh,[2] Vahid Mohammadzadeh,[3] Sakineh Kadivar,[4] and Ali Mohammad Zadeh[5,*]

[1]Department of Biomedical Engineering, Faculty of Advanced Medical Technology, Isfahan University of Medical Sciences, Isfahan, Iran
[2]Department of Radiology, Amiralam hospital, Tehran University of Medical Sciences, Tehran, Iran
[3]Department of Ophthalmology, Farabi Hospital, Tehran University of Medical Sciences, Tehran, Iran
[4]Department of Ophthalmology, Amiralmomenin Hospital, Gilan University of Medical Sciences, Gilan, Iran
[5]Rajaie Cardiovascular Medical and Research Center, Iran University of Medical Sciences, Tehran, Iran

[*]*Corresponding author*: Ali Mohammad Zadeh, Rajaie Cardiovascular Medical and Research Center, Iran University of Medical Sciences, Tehran, Iran. Tel/Fax: +98-2122042026, E-mail: mralimohammadzadeh@yahoo.com

Received 2016 September 19; **Revised** 2016 November 29; **Accepted** 2016 December 19.

Abstract

Background: Left ventricle segmentation plays an essential role in computation of cardiac functional parameters such as ventricular end diastolic and end systolic volumes, ejection fraction, myocardial mass, and wall thickness and also wall motion analysis. Manual segmentation is also time consuming and suffers from inter and intra observer variability. Several approaches have been proposed that segment the left ventricle (LV) by automatic and semi-automatic methods, but the problem is still open due to the huge shape variety of the left ventricle and motion artifact.

Materials and Methods: A robust semi-automatic approach is hereby presented for addressing the left ventricle segmentation problem. The presented method combines region information of the left ventricle with gradient and edge information in a graph framework. The LV region information is captured using our previously presented region growing method and is embedded into livewire framework.

Results: The modified livewire that is presented here shows a great success in quantitative criteria over the publically available MICCAI 2009 left ventricle segmentation challenge database that contains 45 normal and abnormal cases. We have computed dice metric (DM) and average perpendicular distance (APD) for the proposed method and it outperformed the state of the art results over all papers that used the same database. Validation metrics, dice metric and average perpendicular distance were computed as 0.95 mm and 1.48 mm versus those of 0.87 - 0.93 mm and 1.76 - 1.81 mm obtained by other methods, respectively.

Conclusion: Using semi-automatic approaches for cardiac segmentation yields satisfying results and this is because of incorporating radiologist's experiences into the segmentation procedure. Maintaining image information to reduce user interaction is our goal for further researches.

Keywords: Segmentation, Cardiac Magnetic Resonance Imaging, Livewire, Signed Distance Function

1. Background

Cardiac magnetic resonance imaging (CMRI) is an accurate and reproducible technique for the evaluation of cardiac function. It is also the gold standard for ventricular volume measurements as documented by both ex vivo and in vivo studies (1). Left ventricle volume measurement needs segmentation of the left ventricle (LV), which is a difficult task because of its unclear borders and shape variety. The presence of papillary muscles in the ventricle cavity, with gray level values similar to the surrounding myocardium is considered as another problem. In summary, the problem of left ventricle segmentation is still open due to these issues; whereas, numerous methods have been proposed (2, 3). The previous works may be categorized into different groups: active contour (4-6), methods based on computation of thresholding (7, 8), graph search algorithms (9, 10), atlas based methods (11-14), and statistical shape models (active shape and appearance model) (15-17). Among these methods, statistical shape models are the most used approach in this field (2, 3). Atlas-based segmentation uses labeled images, known as atlas, to describe diverse structures present in the intended image. Registration of atlases onto the image to be segmented is the key point of this procedure (3). As literature shows (2, 3), the main drawback of this method is the effect of the registration quality on the success of the approach. Active contour is another approach of medical image segmentation that has been widely used regarding their flexibility (18). Active contours are iteratively deforming curves that minimize an energy functional with their evolution, and meanwhile use information of object boundaries and smooth-

ness of curve as separate terms (2). A number of methods have been worked on using active contour model for left ventricle segmentation. Grosgeorge et al. (5) utilized well-known region based active contour approach, Chan-Vese approach, for segmentation of both left and right ventricle. Their results show a satisfying segmentation, but because of using region term solely, this method results good only in homogenous regions with well-defined borders. Graph based method is another approach used for right and left ventricle segmentation. In graph-based methods, every image pixel is considered as node and edges between graph nodes are defined with similarity function. Cut is a set of edges of graph that omitting them partitions the graph into two disjoint sets. Global optimization of cost function is the framework of this approach. Graph theoretic techniques are not limited to graph cut and generally are categorized into four groups (19): (1) Graph cut: Cuts can be obtained using minimizing a predefined cost function or on Markov random field models. (2) Minimum path based methods: These methods are semi-automatic approaches that define the object frontiers as minimum cost paths between each pairs of nodes. (3) Methods based on minimal spanning tree: A minimum spanning tree (MST) is a tree of a connected undirected graph that connects all the vertices together with the minimal total weights for its edges. For segmentation by this approach, edges from different sub-graphs are removed. (4) Other methods: graph based segmentation methods that are not part of any of the above categories (20). Among these four approaches, minimum path based method is considered as a semi-automatic technique. So, it is more interesting in medical applications because incorporating radiologist knowledge makes the segmentation process more reliable and accurate. The most well-known algorithm for solving "minimum path finding problem" is Dijkstra's algorithm (21), which is also utilized in livewire (22). 2-D livewire method provides the possibility of selecting an initial point on the boundary of the object to be segmented. The next point is placed in a way such that the lowest cost path between the initial point and the current cursor position will find the object of interest interactively. There are efforts for extending 2-D livewire to 3-D framework (23-25) in various applications, especially medical applications. Another extended version of live wire is proposed in a study conducted by Poon et al. (26), in which the cost function is modified so it can segment vessel images more appropriately. They added vesselness filter, vessel direction term and fitness of medial node term to the livewire cost function. This idea actually works well in the 2-D segmentation context. Classical livewire hires image features like edge and gradient information, while this information in the ventricle border is inaccessible more often due to ill-defined borders and partial volume effect.

2. Objectives

We have used a simple region-based shape prior term for representation of the left ventricle. The shape prior, which is named LVness (a term that represents the shape of the LV), is based on a region growing algorithm that we previously presented (27). LVness produces a primary segmentation of the left ventricle according to region information. The resulted border pixels have low intensity values and guide the minimum path search algorithm to the predefined band. In the following, first we will describe the livewire approach and LVness generation procedure. The qualitative and quantitative results of applying proposed method on 45 cases of MRI images of a publically available dataset (MICCAI 2009 left ventricle segmentation challenge) is presented in the next section. Finally, discussion, conclusion and suggestions for future researches are presented in the later section.

3. Materials and Methods

3.1. Livewire

Livewire algorithm is a semi-automatic tool for accurate segmentation that gives the seed from user input. As the user selects seed points, and moves the mouse, optimal boundaries are computed and found. The classic 2-D livewire uses the gradient magnitude $f_m(q)$ gradient direction $f_d(p,q)$, and canny operator $f_c(q)$ for creating cost function from pixel p to pixel q C(p,q) (24).

$$C(p,q) = w_M f_M(q) + w_D f_D(p,q) + w_C f_C(q) \quad (1)$$

Where w_M, w_D and w_C are gradient magnitude, gradient direction, and edge detection weights respectively. These weights provide the possibility of contribution to the cost function with various rates for each cost term. The gradient magnitude is defined as:

$$f_M(q) = 1 - \frac{\sqrt{\left(\frac{dq}{dx}\right)^2 + \left(\frac{dq}{dy}\right)^2}}{\max(G)} \quad (2)$$

In this equation, G refers to gradient magnitude in the 2D image and max (G) represents the largest gradient magnitude. As it is clear, gradient magnitude has high value in borders and low value in homogenous regions. As mouse moves around the object, the border pixels should have low costs so livewire algorithm can tend to the border. It's obvious that gradient magnitude must be inverted and this provides low cost for strong edges. The gradient direction cost term pixel p going to pixel q is defined as:

$$f_D(p,q) = \frac{\arccos\left(\frac{\frac{dp}{dx}}{G(p)} \times \frac{\frac{dq}{dx}}{G(q)} + \frac{\frac{dp}{dy}}{G(p)} \times \frac{\frac{dq}{dy}}{G(q)}\right)}{\pi} \quad (3)$$

Where G(p) represents the gradient magnitude for pixel p. Finally, $f_c(q)$ is the canny edge detector (28). Canny edge detector results a binary image with white pixels (it means 1) representing edges and black pixels (it means 0) are background.

Classical livewire hires image features like edge and gradient information, while this information in the left ventricle border is inaccessible more often due to ill-defined borders of LV in these images. Therefore, we used a shape prior term to be added to the cost function of minimum path search algorithm.

3.2. LVness

Here, we have defined a new term to be added to the cost function and incline the path toward the left ventricle. The new cost function forms as follows:

$$C(p,q) = w_M f_M(q) + w_D f_D(p,q) + w_C f_C(q) + w_{LV} f_{LV} \quad (4)$$

Where w_{LV} indicates the weight of LVness term on the equation. For providing LVness by primary segmentation, we have used our previously presented region-based segmentation approach. First, the user selects a seed in the left ventricle region manually and afterward gray space map is formed.

3.3. Gray Space Map

Gray space map composition contains four major steps:

1) The coordinates and gray level value (V) of a seed is obtained by clicking on the left ventricle region.

2) Pixels that have the same gray level value as the seed and are neighbors of the seed pixel are found.

3) At this step, we define a set of gray levels in the interval [V - D, V + D], D ε {1, 2, ... } and look forward pixels in the neighborhood of the previous step and with gray level value in this interval.

4) Every time D increases, corresponding pixels in gray space map catch a lower label.

So, we have an image with the same size as the original image and pixels that are close to the seed (in terms of spatial and gray level value) are highlighted with higher values. Resulted gray space map is demonstrated in Figure 1.

3.4. LVness Generation

Regarding left ventricle prominence in gray space map, which is because of the homogeneous region of the left ventricle and inhomogeneity between LV cavity and surrounding tissues, a robust method is needed to express left ventricle edges as a weighted map like other terms of classic livewire. We have used the antepenultimate (two before the last) stage of canny edge detector (28), in which the edges are described as a weight of edgeness. The canny edge detector has five steps (28).

1) Image smoothing by applying Gaussian filter in order to remove undesired noises. An example of a Gaussian kernel of size = 5 and σ = 1.4 is represented in the following Equation. The The asterisk denotes a convolution operation.

$$B = \frac{1}{159}\begin{bmatrix} 2 & 4 & 5 & 4 & 2 \\ 4 & 9 & 12 & 9 & 7 \\ 5 & 12 & 15 & 12 & 5 \\ 4 & 9 & 12 & 9 & 4 \\ 2 & 4 & 5 & 4 & 2 \end{bmatrix} * A \quad (5)$$

2) Finding the intensity gradient of the image. The canny algorithm first finds horizontal and vertical gradients (G_x and G_y, respectively) using first derivative operators like Sobel. From this the edge gradient and direction can be determined according to the following Equation:

$$G = \sqrt{G_x^2 + G_y^2}; \theta = \arctan\left(\frac{G_y}{G_x}\right) \quad (6)$$

3) Apply non-maximum suppression, which is an edge thinning technique, to remove pixels that are not considered to be part of an edge. Hence, only thin lines (candidate edges) will remain.

4) Exert double threshold to determine potential edges. After application of non-maximum suppression, there are still some edge pixels caused by noise and gray level variation. In order to throw away these artifacts, it is essential to filter out the edge pixel with the low gradient value and preserve the edge with the high gradient value (29).

5) Hysteresis: canny uses lower and upper thresholds (T_1 and T_2, respectively):

- If: pixelGradient > T_2

Then: the pixel is accepted as an edge.

- If: pixelGradient < T_1

Then: the pixel is rejected.

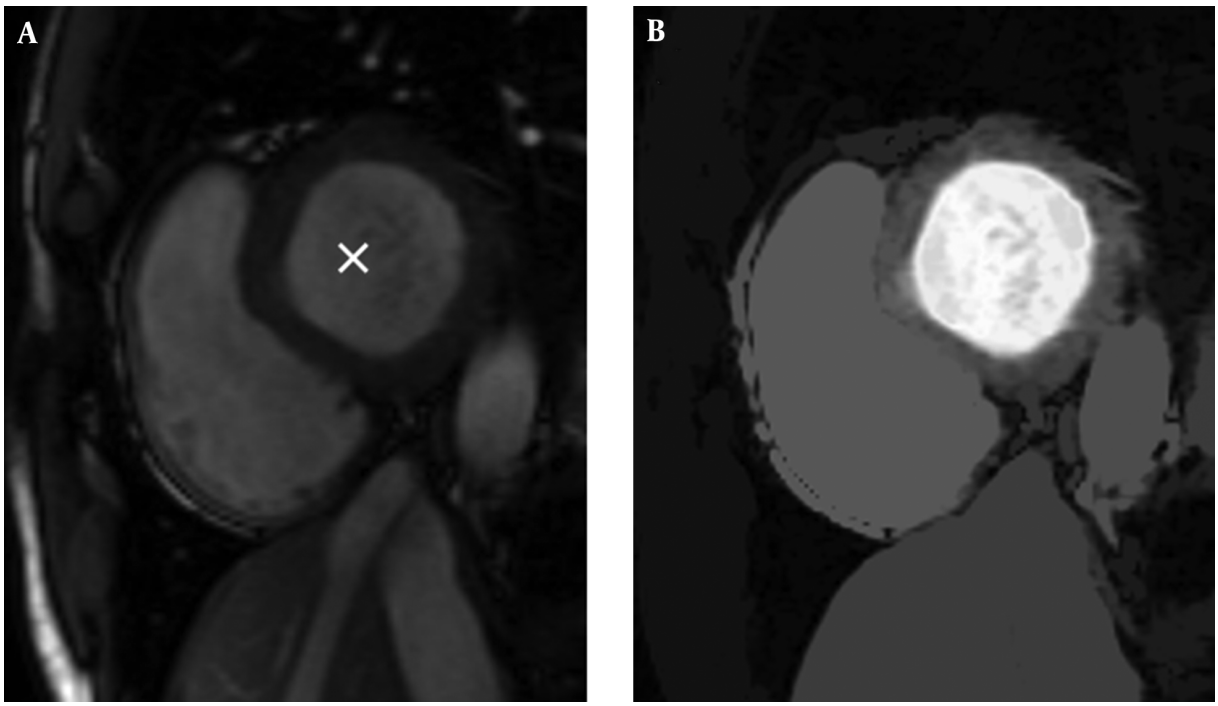

Figure 1. Gray space map with a seed pixel inside the left ventricle. A, The original image with the seed displayed by a cross mark; B, Resulted gray space map.

- If: $T_1 <$ pixelGradient $< T_2$

Then: the pixel will be accepted only if it is connected to a pixel that is above T_2

In these steps, the third step (i.e. non-maximum suppression) produces an image, in which pixels that have a weight according to "being edge" rate and on the other hand, undesirable noises are suppressed. If we stop canny algorithm in this step and use weights of this image as a criterion that represents LV border rate in the mouse-moving path, this output can be our LVness.

There is only another step for preparing our LVness and this would be complementing the resulted image. As Figure 2 shows, result of non-maximum suppression algorithm has higher values in more likely edge pixels and lower values for rest of pixels. For being minimum f_{LV} near the left ventricle borders, it should be complemented as it can be seen in Figure 2.

Like other terms in the classic livewire, this new term is an image that has weights that are low values around the borders and high in the rest of the image pixels. As mathematically described above, all terms of modified livewire are images that would be minimum in the mouse-moving path around the LV border. Non-maximum suppression (NMS) has a derivative nature that arises from directional first order derivatives (G_x and G_y), and these operators has maximum in high variations (likes edges) according to following Equations:

$$\frac{\partial f}{\partial x} = f(x+1) - f(x) \tag{7}$$

$$\frac{\partial f}{\partial y} = f(x+1) - f(y) \tag{8}$$

$$f_{LV} = 1 - f_{NMS} \tag{9}$$

This shows that f_{LV}, which is the complement of NMS, is minimal near the borders.

3.5. Graph Searching Algorithm

Finding a low cost path in our directed graph is the next task. Local costs are assigned to nodes in the graph and then, expansion of a user-selected seed point is accrued and it means that its local cost is added into its neighboring nodes. The next pixel, which is expanded, is the neighboring node with the minimum cumulative cost and the process continues till a "wavefront" is produced that expands in order of minimum cumulative cost (22). Figure 3 illustrates the described algorithm. Figure 3A shows the seed point with a circle around it and initial local cost map.

Figure 3B demonstrates a portion of the total cost after the seed point is expanded. Note that diagonal costs have

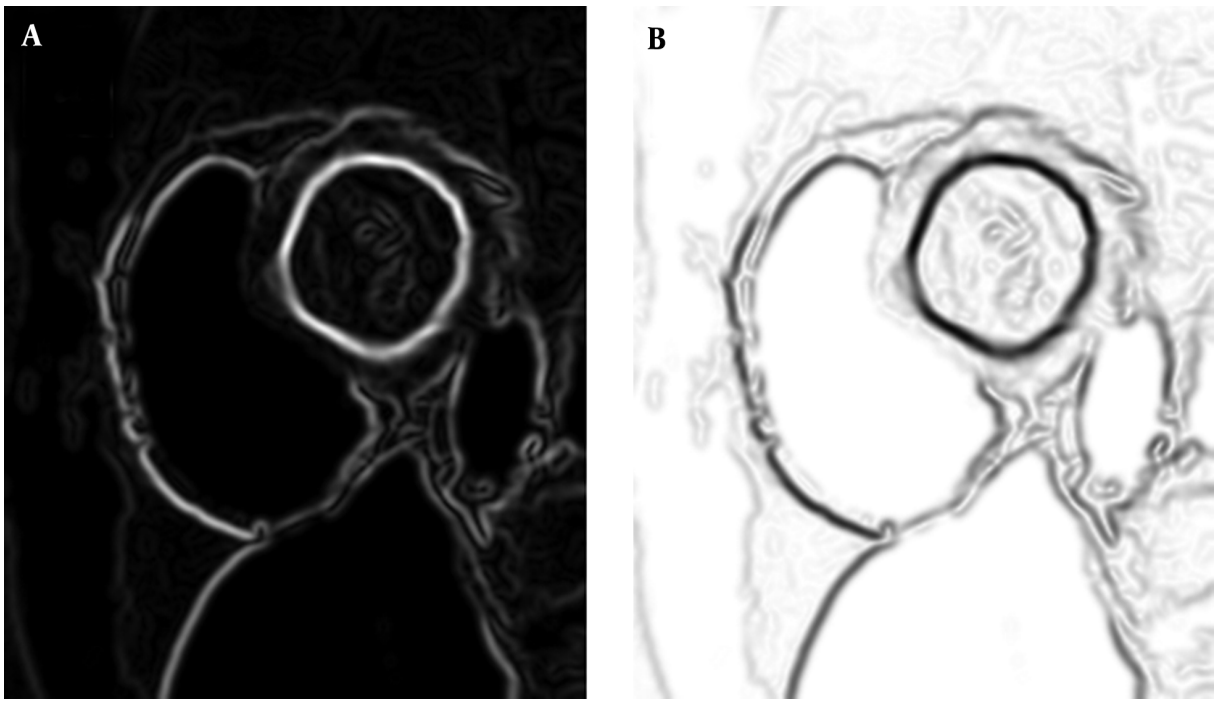

Figure 2. A, Result of third step (non maximal suppression: NMS) of canny edge detector algorithm. B, f_{LV} is the complement of NMS.

been multiplied by Euclidean distance. Figure 3C indicates two points expansion, and Figure 3D-3F show 5, 47 and completed expansion (22).

3.6. Ethical Approval

This article does not contain any studies with human participants or animals performed by any of the authors.

3.7. Informed Consent

Informed consent was obtained from all individual participants included in the study.

4. Results

To evaluate the performance of the proposed method, we applied it to the MICCAI 2009 LV segmentation challenge dataset (3). The database is publicly available online and contains 45 MRI datasets, grouped into three categories. Each category contains 15 cases of ischemic heart failure cases, non-ischemic heart failure cases, LV hypertrophy cases and normal (SC-N) cases. Manual segmentation of images by experts at the end diastole (ED) and the end systole (ES) cardiac phases are available.

4.1. LVness Generation

LVness is built for ED and ES phases of cardiac cycle separately. There are also six LVness models for ED phase from base to apex and six for ES. Livewire cost function terms have weights that are chosen empirically from training sets: $W_M = 0.3$, $W_D = 0.39$, $W_C = 0.17$ and $W_{LV} = 0.14$. These weights are obtained empirically and W_{LV} is set to 0.14 to suppress the effect of LVness in case of possible leakage of GSmap outward of the left ventricle. We have done sensitivity analysis to determine the change in accuracy while varying each weight value (30). We found that varying each weight by $\pm$ 50% did not change the accuracy by more than 4.3% for our test images. For more certainty in this matter, we performed a leave-one-out (LOO) strategy and in each iteration, one of the training, online and validation datasets of the MICCAI 2009 LV segmentation challenge dataset was considered as test group.

4.2. Quantitative and Qualitative Evaluation

Two well-known measures were used to analyze the performance of our segmentation approach with other methods that used dataset (3) dice metric (DM) and average perpendicular distance (APD).

The dice metric is a statistic that measures contour overlap by intersecting automatically segmented area and

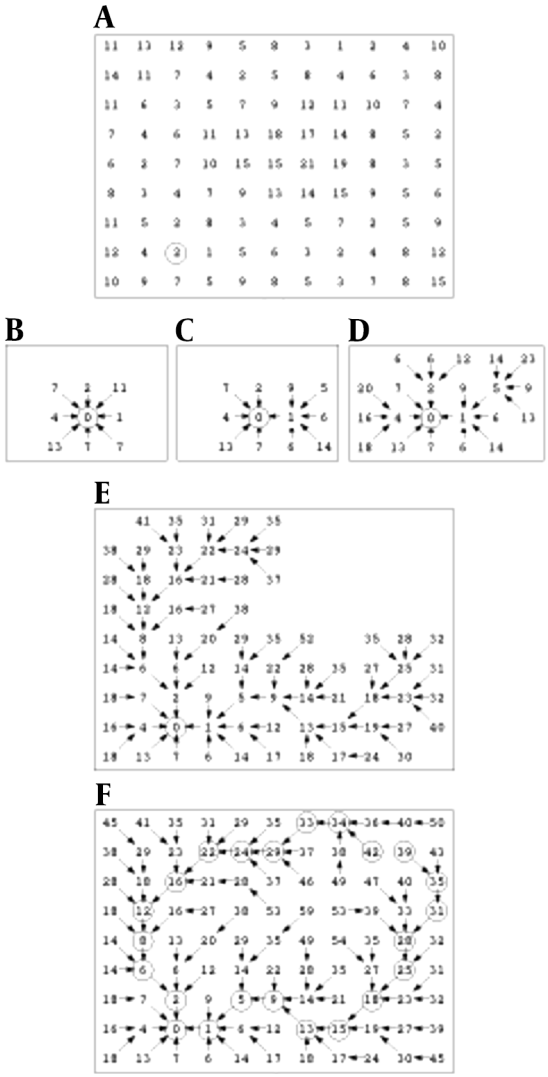

Figure 3. Cost expansion. A, Local cost map. B, Seed point expanded. C, Two points expanded. D, Five points expanded. E, 47 points expanded. F, Completed total cost path/pointer map with optimal paths

manually segmented area , multiplyed by 2, and finally divided by $A_A + A_M$ (3).

$$DM = \frac{2\left(A_A \bigcap A_m\right)}{A_A + A_M} \quad (10)$$

The dice metric is always between zero and one, and higher DM shows better consistency between automated and manual segmentations.

The average perpendicular distance measures the distance from the automatically segmented contour to the corresponding manually drawn expert contour, averaged over all contour points (3). A representation of APD can be seen in Figure 4.

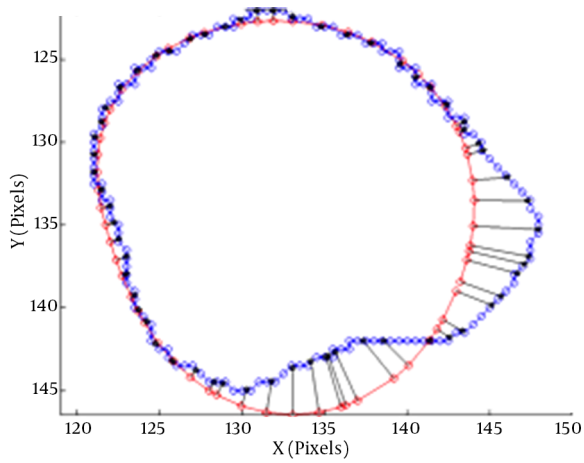

Figure 4. The average perpendicular distance APD between two contours (3)

We have performed our segmentation algorithm on training, validation and online sets of dataset. The qualitative and quantitative tests show promising results. In comparison with other automatic and semi-automatic methods, our proposed method yielded the best results in both gice metric and APD and may be considered as state of the art. Table 1 shows the average values ± the standard deviation of the statistic measurements. Figure 5 illustrates the automatic and manual segmentation results of the LV from the base to the apex and also in ED and ES phases of the cardiac cycle. Segmentation of the left ventricle has pre-mentioned difficulties and these difficulties are boosted in mid and apex slices due to their low resolution and presence of papillary muscle. The ability of our method in segmentation of the left ventricle in these cases is presented in Figure 6.

Table 1. Evaluation Metrics of Our Proposed Method for Training, Validation and Online Sets of Left Ventricle Segmentation Challenge Database (3)[a]

Dataset		DM	APD
Training	ED	0.95 ± 0.26	1.48 ± 1.32
	ES	0.89 ± 0.11	6.23 ± 4.33
Validation	ED	0.92 ± 0.19	4.11 ± 1.19
	ES	0.90 ± 0.12	4.77 ± 0.12
Online	ED	0.88 ± 0.34	3.45 ± 0.79
	ES	0.86 ± 0.29	5.83 ± 2.35

Abbreviations: APD, average perpendicular distance; DM, dice metric; ED, end diastole; ES, end systole.
[a]Values are expressed as mean ± standard deviation.

We have used MATLAB 2015-b with License-number:

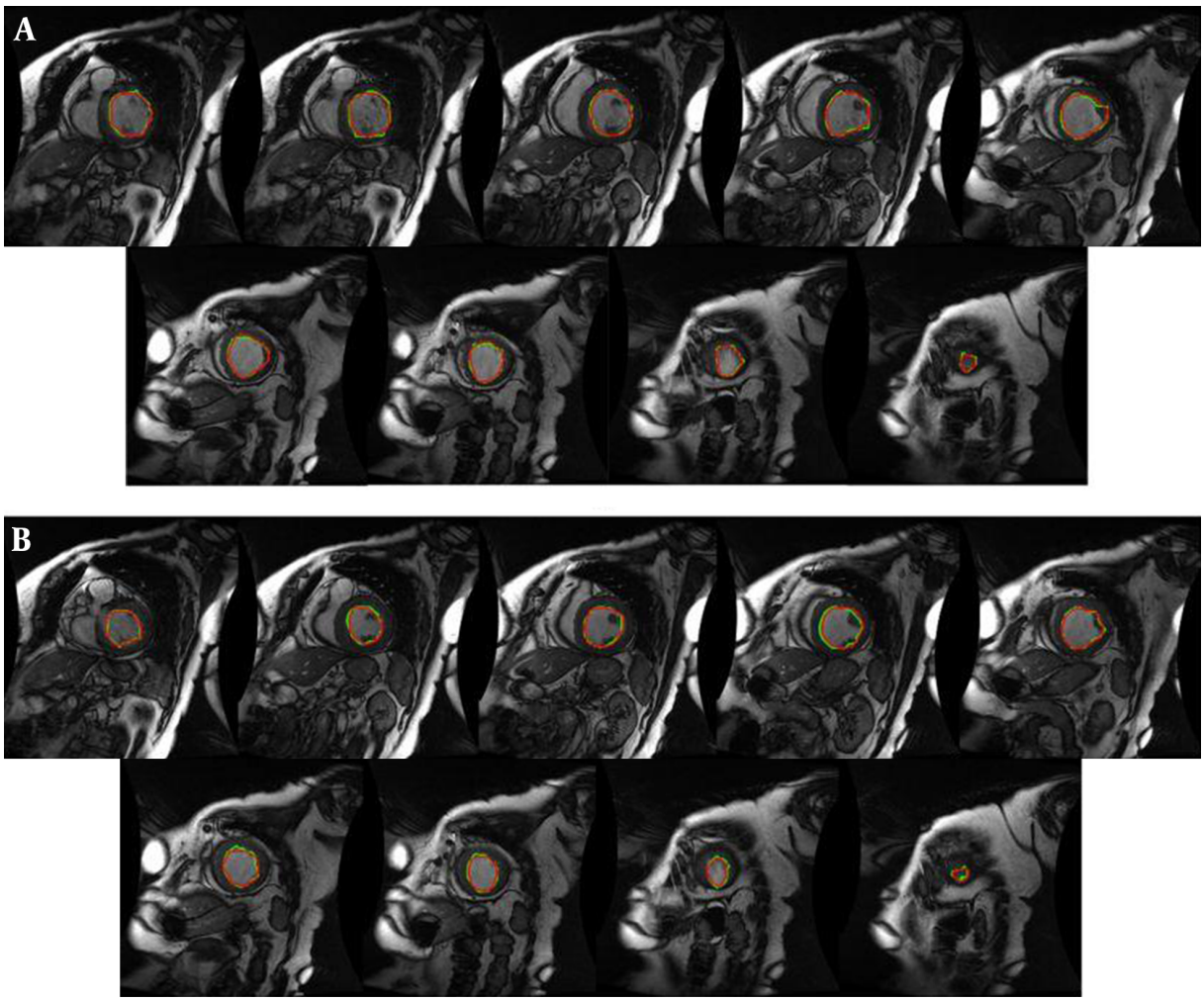

Figure 5. Manual (red) and proposed approach (green) segmentation of the left ventricle from base to apex for an instance case of MICCAI 2009 challenge database (3). A, End diastole; B, End systole.

838860 in a Pentium-4 system with Intel(R) Core(TM) 2 Dou CPU 2.80 GHz 8 GB RAM, 64-bit Windows 7.

5. Discussion

In this study, we developed and validated a new semi-automatic approach for left ventricle segmentation based on 2-D livewire. As classic livewire uses image features like gradient and edge information, and this information is not sufficient or inaccessible in some cases, we used our previously presented region growing algorithm to generate a primary segmentation that could be added as a new term to the livewire equation. Ideally, incorporating all regions, shape and edge information of the left ventricle may produce a fully promising result in left ventricle segmentation. However, incorporating all of these information needs a huge dataset that can capture all the shape varieties in the left ventricle. Computed metrics in Table 1 showed that our approach results provided contours similar to the ground truth by a rate of 93% and improvements in other metrics. Table 2 revealed that our method outperformed the state-of-the-art methods that used the same dataset (3). In Table 2, a comparison of results between our method and the state-of-the-art methods that used the same database is presented. The results show a significant improvement in both dice metric and average perpendicular distance by our proposed method. Figure 5 shows a greet agreement between our proposed method segmentation results and manual segmentation as ground truth. Figure 6 illustrates the ability of proposed method in seg-

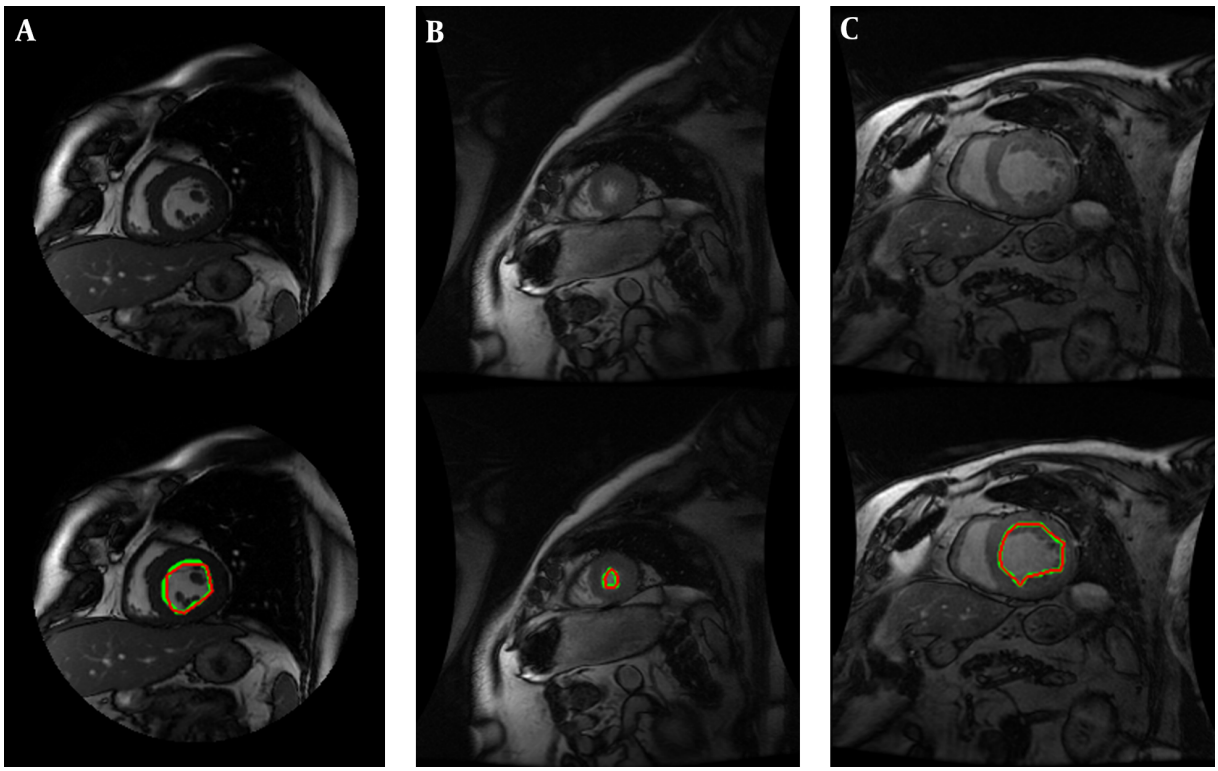

Figure 6. A, Manual (red) and proposed approach (green) segmentation of the left ventricle in some challenging slices containing presence of papillary muscles; B, Apical slices; C, Unclear borders. Top row: original image and bottom row: segmentation result.

mentation of the left ventricle along with whole slices of end diastolic and end systolic phases of the cardiac cycle. In this figure, manual segmentation is declared by red contours and livewire segmentation by green contours. The conformity of manual and livewire segmentation can obviously be seen in all frames.

The most challenging slices for cardiac MRI segmentation could be divided in three groups:

1) Apical slices,

2) Slices with strong papillary muscles

3) Slices with an unclear border.

Figure 6 shows the robustness of the proposed method in segmentation of these challenging slices.

Figures 7 and 8 illustrate the correlation graphs using online data set between our approach and manual results for end diastolic and end systolic volumes, respectively. A correlation with manual segmentation of 0.997 and 0.997 for end-diastolic volume (EDV) and end-systolic volume (ESV) was calculated. The correlation test is obtained using "Pearsons test" to obtain the slope, intercept and the R-values. This high correlation proves the accuracy and clinical applicability for evaluation of LV function.

We used a 2-D approach for segmentation of the left

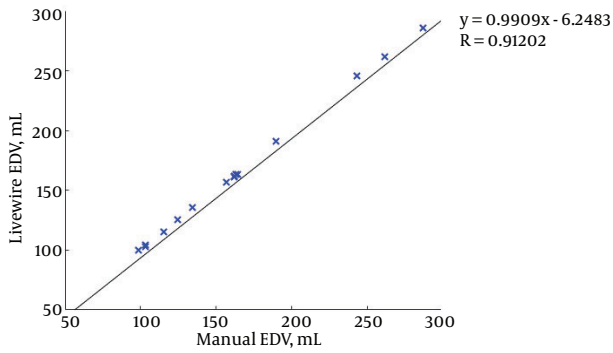

Figure 7. Correlation graph for end-diastolic volume (EDV)

Table 2. Comparison of Segmentation Performance Between Proposed Method and State-Of-The-Art Techniques Using Left Ventricle Segmentation Challenge Database (3) and Other Methods That Used the Same Database[a]

Method	DM	APD
Proposed method	0.95 ± 0.26	1.48 ± 1.32
Classic livewire (22)	0. 88 ± 0.22	8.13 ± 3.87
Oghli et al. 2013 (31)	0.79 ± 0.33	9.12 ± 1.23
Oghli et al. 2012 (32)	0.73 ± 0.56	9.58 ± 2.19
(Queiros et al. 2014) (33)	92.7 ± 0.23	10.51 ± 9.17
(Ngo and Carneiro, 2014) (34)	93.23 ± 0.34	22.20 ± 21.74
(Hu et al. 2013) (35)	0.61 ± 0.29	15.08 ± 8.91
(Constantinides et al. 2012) (36)	0.80 ± 0.19	9.79 ± 5.38
(Jolly et al. 2009) (37)	0.88 ± 0.04	2.97 ± 0.38
(Liu et al. 2012) (38)	0.78 ± 0.20	9.26 ± 4.93
(Huang et al. 2011) (39)	0.81 ± 0.16	7.28 ± 3.58
(Schaerer et al. 2010) (40)	0.77 ± 0.16	9.64 ± 4.15

Abbreviations: APD, average perpendicular distance; DM, dice metric.
[a]Values are expressed as mean ± standard deviation.

ventricle; whereas, 3D methods are becoming the state-of-the-art in medical applications, and this is because of two reasons:

1) The large gap between slices in short axis and other views (about 7 mm) and impossibility of the pixel intensity value estimation in the gaps (2, 3).

2) Misalignment between slices due to motion artifacts in cardiac MRI (25). This means that the cavity center is not at the same position in different slices.

Among various methods that are used for left ventricle segmentation in the literatures, active contour methods (especially level set based method) and active shape and appearance methods (active shape model (ASM) and active appearance model (AAM) are the mostly used approaches. Level set based methods uses an initial contour and aggregate edge information (and in some cases like Chan-Vese region information) to minimize a function that leads to evolve a curve to fit on object boundaries. Besides their significant advantages, these methods have the following limitations:

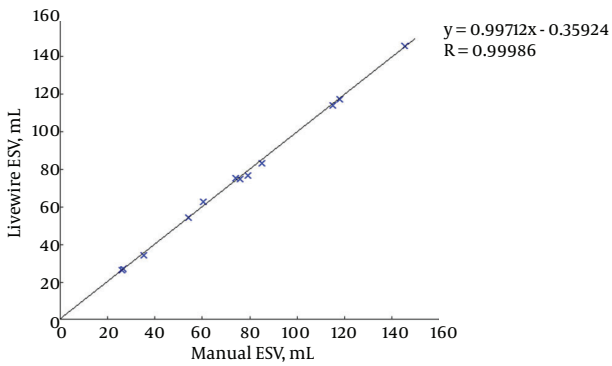

Figure 8. Correlation graph for end-systolic volume (ESV)

1) The main disadvantage of this approach is the dependence of segmentation result to precision of initial contour selection. Although this weakness is mostly resolved, the problem is still open.

2) They can often get stuck in local minimal states; this may be overcome by using simulated annealing techniques, which is the cause of computational complexity.

3) Accuracy is governed by the convergence criteria, which is used in the energy minimization technique. Higher accuracy require tighter convergence criteria and hence, longer computation times.

4) Another issue that makes the use of level set methods for LV segmentation inappropriate is the presence of papillary muscles with gray levels similar to surrounding myocardium. These little circle shaped muscles (which are obvious in Figure 5A) create local minima for evolving curve because of edges that are between them and LV cavity.

It is notable that although the proposed method (base on livewire framework) is a semi-automatic approach as level set method, there are some differences between user interaction in the proposed method and level set approach. The main difference is that in livewire method, user selects the seeds exactly on the left ventricle border and since the operators are expert (or at least semi-expert) they recognize ventricle positions and user interaction will not result in miss-segmentation or user faults. On the other hand, the shortest path between two seeds is recognized based on livewire algorithm and is confirmed by selecting the next seed by the user. While, in the level set method user selects an initial contour and the contour evolves based on an energy minimization algorithm. This fact limits the supervision of the user and may lead to miss-segmentation in some cases.

Active shape and appearance methods hire a point correspondence based method [point distribution model (PDM)] for representation of left or right ventricle shape. ASM captures shape variations, constructs a model and aims to match the model to a new image. On the other hand, AAM works with shape and appearance of object simultaneously based on correspondent points (15). The main drawback of these techniques is the dependence of the result of segmentation on the similarity of shapes to the training set.

5.1. Conclusions

In summary, a combined semi-automatic approach for segmentation of the left ventricle is proposed in this paper, which incorporates region information with a region-growing algorithm into the livewire framework. In contrast to automatic manners, semi-automatic approaches in image segmentation has the advantage of using knowledge and experience of a radiologist. This superiority is more essential in cardiac MRI image analysis, which has a lot of ambiguities in interpretation of the image. On the other hand, the time spent for segmentation of a single slice is very lower than manual segmentation.

Acknowledgments

The authors like to thank Dr. Maleki for his valuable support.

Footnotes

Authors' Contributions: Study concept and design: Mostafa Ghelich Oghli; acquisition of data: Maryam Mohammadzadeh; analysis and interpretation of data: Mostafa Ghelich Oghli and Sakineh Kadivar; critical revision of the manuscript for important intellectual content and study supervision: Ali Mohammadzadeh; statistical analysis: Vahid Mohammadzadeh

Funding/Support: This study was funded by Rajaei cardiovascular medical and research center.

Conflict of Interest: There is no conflict of interest.

Financial Disclosure: There is no financial disclosure.

References

1. Sarwar A, Shapiro MD, Abbara S, Cury RC, editors. Cardiac magnetic resonance imaging for the evaluation of ventricular function. Seminars in roentgenology. 2008; Elsevier; pp. 183–92.
2. Petitjean C, Dacher JN. A review of segmentation methods in short axis cardiac MR images. *Med Image Anal.* 2011;**15**(2):169–84. doi: 10.1016/j.media.2010.12.004. [PubMed: 21216179].
3. Radau P, Lu Y, Connelly K, Paul G, Dick A, Wright G. Evaluation framework for algorithms segmenting short axis cardiac MRI. *MIDAS J Cardiac MR Left Ventricle Segment Challenge.* 2009;**49**.
4. Pluempitiwiriyawej C, Moura JMF, Wu YJL, Ho C, editors. Cardiac MR image segmentation: quality assessment of STACS. Biomedical Imaging: Nano to Macro, 2004. IEEE International Symposium on. 2004; IEEE; pp. 828–31.
5. Grosgeorge D, Petitjean C, Caudron J, Fares J, Dacher JN. Automatic cardiac ventricle segmentation in MR images: a validation study. *Int J Comput Assist Radiol Surg.* 2011;**6**(5):573–81. doi: 10.1007/s11548-010-0532-6. [PubMed: 20848320].
6. Pluempitiwiriyawej C, Moura JM, Wu YJ, Ho C. STACS: new active contour scheme for cardiac MR image segmentation. *IEEE Trans Med Imaging.* 2005;**24**(5):593–603. doi: 10.1109/TMI.2005.843740. [PubMed: 15889547].
7. Katouzian A, Prakash A, Konofagou E. A new automated technique for left-and right-ventricular segmentation in magnetic resonance imaging. Engineering in Medicine and Biology Society. 28th Annual International Conference of the IEEE. IEEE; .
8. Lin X, Cowan BR, Young AA, editors. Automated detection of left ventricle in 4D MR images: experience from a large study. International Conference on Medical Image Computing and Computer-Assisted Intervention. 2006; Springer; pp. 728–35.
9. Grosgeorge D, Petitjean C, Dacher JN, Ruan S. Graph cut segmentation with a statistical shape model in cardiac MRI. *Comput Vision Image Understand.* 2013;**117**(9):1027–35. doi: 10.1016/j.cviu.2013.01.014.
10. Lee HY, Codella N, Cham M, Prince M, Weinsaft J, Wang Y. Left ventricle segmentation using graph searching on intensity and gradient and a priori knowledge (lvGIGA) for short-axis cardiac magnetic resonance imaging. *J Magn Reson Imaging.* 2008;**28**(6):1393–401. doi: 10.1002/jmri.21586. [PubMed: 19025947].
11. Zuluaga MA, Cardoso MJ, Modat M, Ourselin S. Multi-atlas propagation whole heart segmentation from MRI and CTA using a local normalised correlation coefficient criterion. International Conference on Functional Imaging and Modeling of the Heart. Springer; .
12. Ou Y, Sotiras A, Paragios N, Davatzikos C. DRAMMS: Deformable registration via attribute matching and mutual-saliency weighting. *Med Image Anal.* 2011;**15**(4):622–39. doi: 10.1016/j.media.2010.07.002. [PubMed: 20688559].
13. Zhuang X, Hawkes DJ, Crum WR, Boubertakh R, Uribe S, Atkinson D, et al, editors. Robust registration between cardiac MRI images and atlas for segmentation propagation. Medical Imaging. 2008; International Society for Optics and Photonics; pp. 691408–691408-11.
14. Lorenzo-Valdes M, Sanchez-Ortiz GI, Elkington AG, Mohiaddin RH, Rueckert D. Segmentation of 4D cardiac MR images using a probabilistic atlas and the EM algorithm. *Med Image Anal.* 2004;**8**(3):255–65. doi: 10.1016/j.media.2004.06.005. [PubMed: 15450220].
15. Mitchell SC, Lelieveldt BP, van der Geest RJ, Bosch HG, Reiber JH, Sonka M. Multistage hybrid active appearance model matching: segmentation of left and right ventricles in cardiac MR images. *IEEE Trans Med Imaging.* 2001;**20**(5):415–23. doi: 10.1109/42.925294. [PubMed: 11403200].
16. Ordas S, Boisrobert L, Huguet M, Frangi AF, editors. Active shape models with invariant optimal features (IOF-ASM) application to cardiac MRI segmentation. Computers in Cardiology, 2003. 2003; IEEE; pp. 633–6.
17. Lotjonen J, Kivisto S, Koikkalainen J, Smutek D, Lauerma K. Statistical shape model of atria, ventricles and epicardium from short- and long-axis MR images. *Med Image Anal.* 2004;**8**(3):371–86. doi: 10.1016/j.media.2004.06.013. [PubMed: 15450230].
18. Xu C, Pham DL, Prince JL. Image segmentation using deformable models. Handbook of medical imaging. ; 2000. pp. 129–74.
19. Peng B, Zhang L, Zhang D. A survey of graph theoretical approaches to image segmentation. *Pattern Recognit.* 2013;**46**(3):1020–38. doi: 10.1016/j.patcog.2012.09.015.
20. Grady L, editor. Multilabel random walker image segmentation using prior models. 2005 IEEE Computer Society Conference on Computer Vision and Pattern Recognition (CVPR'05). 2005; IEEE; pp. 763–70.
21. Dijkstra EW. A note on two problems in connexion with graphs. *Numerische Mathematik.* 1959;**1**(1):269–71. doi: 10.1007/bf01386390.
22. Barrett WA, Mortensen EN. Interactive live-wire boundary extraction. *Med Image Anal.* 1997;**1**(4):331–41. [PubMed: 9873914].
23. Falcao AX, Udupa JK, editors. Segmentation of 3D objects using live wire. Medical Imaging 1997. 1997; International Society for Optics and Photonics; pp. 228–35.
24. Hamarneh G, Yang J, McIntosh C, Langille M. 3D live-wire-based semi-automatic segmentation of medical images. Medical imaging. International Society for Optics and Photonics; 2005.

25. Liew YM, McLaughlin RA, Chan BT, Abdul Aziz YF, Chee KH, Ung NM, et al. Motion corrected LV quantification based on 3D modelling for improved functional assessment in cardiac MRI. *Phys Med Biol.* 2015;**60**(7):2715–33. doi: 10.1088/0031-9155/60/7/2715. [PubMed: 25768708].
26. Poon K, Hamarneh G, Abugharbieh R. Live-vessel: Extending livewire for simultaneous extraction of optimal medial and boundary paths in vascular images. International Conference on Medical Image Computing and Computer-Assisted Intervention. Springer; .
27. Oghli MG, Fallahi A, Pooyan M. Automatic region growing method using GSmap and spatial information on ultrasound images. 18th Iranian Conference on Electrical Engineering. IEEE; .
28. Canny J. A computational approach to edge detection. *IEEE Trans Pattern Anal Mach Intell.* 1986;**8**(6):679–98. [PubMed: 21869365].
29. Otsu N. A threshold selection method from gray-level histograms. *Automatica.* 1975;**11**(285-296):23–7.
30. Glaser BG. Theoretical sensitivity: Advances in the methodology of grounded theory. Sociology Pr; 1978.
31. Oghli MG, Fallahi A, Dehlaghi V, Pooyan M. Left ventricle volume measurement on short axis mri images using a combined region growing and superellipse fitting method. *Int J Signal Image Proc.* 2013;**4**(2).
32. Oghli MG, Fallahi A, Dehlaqi V, Pooyan M, Abdollahi N. A Novel Method for Left Ventricle Volume Measurement on Short Axis MRI Images Based on Deformable Superellipses. International Joint Conference on Advances in Signal Processing and Information Technology. Springer; .
33. Queiros S, Barbosa D, Heyde B, Morais P, Vilaca JL, Friboulet D, et al. Fast automatic myocardial segmentation in 4D cine CMR datasets. *Med Image Anal.* 2014;**18**(7):1115–31. doi: 10.1016/j.media.2014.06.001. [PubMed: 25042098].
34. Anh Ngo T, Carneiro G. Fully automated non-rigid segmentation with distance regularized level set evolution initialized and constrained by deep-structured inference. Proceedings of the IEEE Conference on Computer Vision and Pattern Recognition. .
35. Hu H, Liu H, Gao Z, Huang L. Hybrid segmentation of left ventricle in cardiac MRI using Gaussian-mixture model and region restricted dynamic programming. *Magn Reson Imaging.* 2013;**31**(4):575–84. doi: 10.1016/j.mri.2012.10.004. [PubMed: 23245907].
36. Constantinides C, Roullot E, Lefort M, Frouin F. Fully automated segmentation of the left ventricle applied to cine mr images: description and results on a database of 45 subjects. 2012 Annual International Conference of the IEEE Engineering in Medicine and Biology Society. IEEE; .
37. Jolly M. Fully automatic left ventricle segmentation in cardiac cine MR images using registration and minimum surfaces. *MIDAS J Cardiac MR Left Ventricle Segment Challenge.* 2009;**4**.
38. Liu H, Hu H, Xu X, Song E. Automatic left ventricle segmentation in cardiac MRI using topological stable-state thresholding and region restricted dynamic programming. *Acad Radiol.* 2012;**19**(6):723–31. doi: 10.1016/j.acra.2012.02.011. [PubMed: 22465463].
39. Huang S, Liu J, Lee LC, Venkatesh SK, Teo LL, Au C, et al. An image-based comprehensive approach for automatic segmentation of left ventricle from cardiac short axis cine MR images. *J Digit Imaging.* 2011;**24**(4):598–608. doi: 10.1007/s10278-010-9315-4. [PubMed: 20623156].
40. Schaerer J, Casta C, Pousin J, Clarysse P. A dynamic elastic model for segmentation and tracking of the heart in MR image sequences. *Med Image Anal.* 2010;**14**(6):738–49. doi: 10.1016/j.media.2010.05.009. [PubMed: 20598934].